1-26-2024

ANALYZING NOVEL METAL ALLOYS FOR GLUCOSE SENSING AND ELECTROCATALYSIS

Anna Grace Boddy
Rowan University

ANALYZING NOVEL METAL ALLOYS FOR GLUCOSE SENSING AND ELECTROCATALYSIS

by

Anna G. Boddy

A Thesis

Submitted to the
Department of Chemistry and Biochemistry
College of Science and Mathematics
In partial fulfillment of the requirement
For the degree of
Master of Science in Pharmaceutical Sciences
at
Rowan University
November 30, 2023

Thesis Chair: Erik P. Hoy, Ph.D., Assistant Professor, Department of Chemistry and Biochemistry

Committee Members:
Amos Mugweru, Ph.D., Professor, Department of Chemistry and Biochemistry
Kandalam V. Ramanujachary, Ph.D., Professor, Department of Chemistry and Biochemistry

Dedications

I want to dedicate this work to my family, my father, Paul, and my sister, Angela. Without them, I wouldn't be able to achieve my goals and be where I am at. I would also like to dedicate this work to my significant other, Jimmy, who supported me throughout my college experience.

I would also like to show appreciation to my close friends who are like family, and who were there for me during this journey. Through the program, they showed unconditional love and support when I needed it.

Acknowledgments

I would like to express my absolute appreciation to Professor Erik P. Hoy for taking me in as his graduate student and learning plenty of resourceful knowledge from him. With his help, I was able to format my project and complete my thesis, even when problems occurred. With the knowledge from the last two years, I will be able to tackle any challenges that are presented to me. Thank you to everyone else in the Hoy research group, who assisted me when needed too.

Abstract

Anna G. Boddy
ANALYZING NOVEL METAL ALLOYS FOR GLUCOSE SENSING AND ELECTROCATALYSIS
2022-2023
Erik P. Hoy, Ph.D.
Master of Science in Pharmaceutical Sciences

In pharmaceutical and medicinal chemistry, metals and metal alloys often receive less attention compared to biological or organic compounds due to many factors including toxicity in the body for drug development or the cost of these metals. However, metals can play an important role in pharmaceuticals, having an impact on original cancer drugs, such as platinum used for head and neck tumors. Electrocatalysis is also another topic that receives less attention over topics such as chromatography in pharmaceuticals due to its potential toxic catalysts and voltages that could be harmful to the body. Electrocatalytic sensors can play an important role in pharmaceuticals by measuring concentrations of biomolecules. In this case, an electrocatalytic reaction was studied, catalyzing CO_2 into DMC for laboratory purposes. This electrocatalytic reaction used an Au/Pd slab catalyzing CO_2 to DMC while determining its mechanism computationally. With the knowledge of sensors and metal alloys, potential glucose sensors were studied with three different types of Nickel Phosphides (NiPs) to determine how effective each is in sensing applications based on the metal content, binding energies, Fermi energies, and binding of other biomolecules in blood. This work was fully computational, with a checkerboard Au/Pd slab being efficient for CO2 electrocatalysis and Ni_3P being the most desirable glucose sensor out of all three. The software consists of Schrodinger, Quantum Espresso, and the Amsterdam Modeling Suite.

Table of Contents

Table of Contents (Continued)

List of Figures

List of Tables

Table Page

Chapter 1

Introduction

1.1 Solid-State Metals in Pharmaceuticals

1.1.1 Solid-State Metals and Their Impact on Pharmaceuticals

In pharmaceutical chemistry, metals play an important role due to their properties and binding. However, metals are often overlooked in the pharmaceutical world compared to organic counterparts and the thought of toxicity of metals in the body. Some properties that metals can provide that organics cannot include charge variation, metal complexes, ligand interaction, Lewis Acid properties, redox activity, and their partially filled D shells which can contribute different properties (Paul, 2019). Metal complexes differ in charge variation because of their abilities to bind to positively or negatively charged biomolecules, and that the complex's charges can be modified. When metals bind to ligands, that can make a biological reaction more spontaneous. The structure and binding of these metals can be determined by oxidation state and metals can be modified into different complexes. The Lewis Acid properties allow for polarizability and metals can activate substrates for Redox reactions. Lastly, the partially filled D and F orbitals can play a role in transition metals that can influence different properties. (Paul, 2019) Some metals that have been extensively studied are platinum and other transition metals, in addition to lithium and some other first and second-group metals. Platinum was used as one of the first cancer drugs, as Cisplatin, which was prevented usage later on due to toxicity, but started extensive studies on transition metals and anticancer drugs (Paul, 2019). Another metal of interest is lithium, which has shown effectiveness in manic-

depressive drugs. Overall, metals in pharmaceutical chemistry should not be overlooked because they can make a difference in many different applications.

1.1.2 Metals in Glucose Sensing

Metals contribute tremendously to pharmaceuticals, including glucose sensing, which is the main investigation in this thesis. In glucose sensing, the overall goal is to measure the concentration of glucose or a product of glucose in a reaction to determine the levels of glucose in the body of a diabetic patient. To do so, there are different techniques on how to capture and react glucose, but the main focus will be chemisorption on metals since this was a preliminary investigation into different properties of metal alloys and if they would be substantial in further studies. Chemisorption is adsorbing glucose onto an electrode and running the reaction on the surface (Naikoo et al., 2021). To create these electrode-like surfaces, metals are commonly used as non-enzymatic glucose sensors (NEGS). Some common metals involved in NEGS are Co, Ni, Cu, Zn, and other transition metals (Naikoo et al., 2021). These are involved due to their electrocatalytic abilities, stability, and other metal-like properties that would aid in catalysis. In many cases, there are metal alloys, such as bi-metal alloys and even metal/nonmetal alloys that help aid because of their catalytic abilities. Some examples include oxides, sulfides, and phosphides. The focus will be phosphides with nickel, due to their thermodynamic stability, superior electrical conductivity , and other properties that make it a great catalyst. For example, Laursen et. al introduced nickel phosphides like Ni_5P_4 requires no conductive support and NiPs are more stable due to less corrosion with the formation of the Ni-P amorphous slab (Anders B. Laursen, 2018). These

properties indicate that nickel phosphides can react easily and won't break down in reaction as much as, for example, nickel on its own.

1.2 Introduction to Electrocatalysis

1.2.1 Metals in Electrocatalysis

In electrocatalytic reactions, reactants undergo a chemical process to form products supported by electrochemical techniques such as catalysts and voltages. In a general chemistry sense, catalysts can lower an activation energy hump that the reactants need to go over and become more spontaneous. Electrocatalysis is practical in all types of chemistry and biochemistry, including organic synthesis, pharmaceutical mediators, and environmental resources [5, 12]. The catalysts themselves can range from organic to inorganic, which can be highly influenced by what's needed, where it's happening, and the scale of the reaction. The main focus in this work is metal alloys, due to their conductive properties and ionic bonding properties. In environmental resources, CO_2 catalysis and HER catalysis are two in-demand options due to global warming and the potential usage of H_2 renewal for energy usage [5]. Metal alloys are important in organic synthesis and pharmaceuticals as well, for example platinum, playing an important role in catalysts and cancer drugs (Paul, 2019). However, other metal alloys are efficient in glucose sensing and other types of pharmaceutical sensing, such as transition metals, due to their catalytic properties and lower cost compared to platinum, but still have that conductivity for the voltaic system.

1.2.2 CO_2 Electrocatalysis

In the environmental world, CO_2 is a greenhouse gas that has been an influence in global warming for years due to its negative impacts on the Earth (Masson-Delmotte, 2021). Due to its gaseous nature, different techniques of CO_2 capture and catalysis have been tried, and some are useful, but not effective for large-scale solutions. Currently, some transition metal alloys have been of interest due to their conductivity, such as Sn, Ni, Au, and Pd [6, 7, 9, 13]. As catalysts, these transition metals have shown effectiveness in capturing and releasing different products that can be useful in a laboratory, such as methanol or formic acid [6]. This process could be useful for removing CO_2 from the atmosphere, providing new sources of industrial precursior chemical, and providing part of the solution to our global climate crisis. However, as stated before, these reactions cannot be taken to a larger scale. That is partially due to a high cost, low spontaneity, excessive conditions, or low product [6, 7]. So, the objective would be to prepare an electrocatalyst that would yield plenty of products with reasonable conditions. In this work, an electrocatalytic reaction was done with an Au/Pd alloy to form DMC. The properties of both of these metals contribute great catalytic abilities to catalyze CO_2 to DMC.

1.2.3 Electrocatalysis and Its Impact on Pharmaceuticals

Electrocatalysis has been significant in many different concepts of chemistry and biochemistry. One of them, being pharmaceuticals. Key electrocatalytic techniques in pharmaceuticals include sensors, which can help detect or determine the concentration of a drug or a biomolecule. For example, the pH levels or nitrite levels from a sensor can

help determine if someone has a urinary tract infection (UTI) [12]. Another applicable example includes the detection of a CA mismatch in DNA-CT for the use of a site-specific drug called daunomycin [15]. The main focus of this work, however, is glucose sensing.

1.3 Computational Methods

1.3.1 DFT

Time Independent Density Functional Theory (DFT) is the main technique used for these computational simulations for electrocatalytic mechanisms and glucose sensing. DFT is a quantum mechanical method used to calculate structures along with other properties in computational chemistry and physics (Tanja van Mourik, 2014). Time independant DFT reformulates the Schrodinger equation ($\hat{H}\Psi=E\Psi$) in terms of the electron density and is simplified with the Born-Oppenheimer approximation by separating electronic and nuclear motions with corrections (Tanja van Mourik, 2014). There are plenty of components to be optimized/included in modern DFT calculations such as dispersion correction, self-consistent functions, basis sets, and functionals (M. Bursch, 2022). These functionals are varied and can range in complexity depending on the number of components added. Each calculation also requires defining a basis set which is a series of functions that represent an atomic or molecular orbital. The number of these basis functions and the number of electrons determines the size and time cost of the calculation depending on the space spanned by the basis set of that calculation (Tanja van Mourik, 2014). Through years of study, the functionals and basis sets can vary in size and even be specific to metals, organic molecules, etc. Metals might use simpler

functionals and basis sets compared to an organic reaction, however. Size and structure play an important factor. Other DFT components that can be added include electronic, vibrational, density of states (DOS), and other properties to calculate needed properties (Tanja van Mourik, 2014). In most of this work, geometry optimizations are done, which determine the minimum energy of the system by using DFT. Transition states (TS) are also done, which are a maximum energy calculation with DFT. The geometry optimizations just represent the most likely case of how a system would exist in the given conditions while TS is a common general chemistry topic of the "in-between" reactants and products. Overall, computational optimizations are used to determine mechanisms of reactions, total energies, and other data that can be compared to experimental results or function on their own.

1.3.2 Solid-State DFT

In solid-state DFT, this involves solid-state materials, as the name suggests, such as metals in slabs, which is the focus of all the work in this thesis. This type of DFT can give knowledge of surface chemistry and physics based on periodic systems. Some properties that can be included in the solid state include structural, chemical, optical, spectroscopic, elastic, vibrational, and thermodynamic properties (Tanja van Mourik, 2014). In these simulations, the system of interest is in a unit cell, which is a periodic system that's represented in multiple copies surrounding that unit cell. For example, a solid metal atom is surrounded by a structured lattice of other metal atoms, which would give a good visual idea of how these unit cells are placed. To calculate the properties of this reaction in the unit cell, DFT is done with different components. Solid state calculations include K points, which is an overall sum of the reciprocal space, which this

K space is perpendicular to the real space (Hassan, 2015; Peter Kratzer, 2019). In this work, the solid-state software, Quantum Espresso is used in Schrodinger software. In the optimizations used in AMS software, they are also solid state (R. Rüger, 2023).

In AMS, DFTB (Density Functional Tight Binding) calculations were done to replace DFT in the electrocatalysis studies for larger-scale simulations. DFTB has more approximations than DFT, allowing for these larger-scale simulations.

Chapter 2

Glucose Sensing With Nickel Phosphides

2.1 Introduction

Diabetes, or Diabetes Mellitus, is a disease that is caused by improper levels of insulin in the body. This is caused by not producing enough insulin (type 1) or not using the insulin properly (type 2) (Emerging Risk Factors Collaboration 1; N Sarwar, 2010). In the body, most of the food that's consumed is broken into sugar or glucose. This glucose is used for energy and is transported through the blood stream and insulin is needed for this transport into different cells for energy. However, insulin is produced in the pancreas and if that's not being produced properly, glucose remains in the bloodstream, causing an imbalance of glucose in the bloodstream (Emerging Risk Factors Collaboration 1; N Sarwar, 2010; Pandey, 2011). Too much glucose in the bloodstream can result in high blood sugar. Without being treated, that can result in hyperglycemia, hypoglycemia, or other metabolic problems for the patient. For those who have either type of Diabetes, a glucose monitor of some sort is needed, which can be used to detect glucose levels in the body to determine if the patient's glucose levels are too high or too low, to prevent any complications, and to treat the patient properly. There are many different pathways and processes in glucose sensing mechanisms due to different enzymes in the body that metabolize glucose for energy. A glucose monitor will detect glucose or something similar that is proportional to the concentration of glucose by absorbing it to the surface of the monitor. Glucose monitors have been around since 1962 (Leland C. Clark, 1962) and have been vastly studied since. Glucose sensors need

improvement, however, especially with the cost of expensive metals in the sensor, the effectiveness of the sensor, and how often the glucose is being detected in many cases. Glucose monitors and other sensors work similarly to an electrocatalytic reaction, trying to detect the glucose levels through chemisorption. In these computational studies, the slabs of interest aren't acting as sensors, but based on their binding and electron transfer efficiency. Glucose monitors tend to be detected in blood, but other interstitial fluids have been studied additionally. Since blood is the most commonly used in typical glucose monitors, the healthy patient would have a blood glucose range of 4.9-6.9 mM, and a diabetic patient could go up to 40 mM (Association, 2007; Danielle Bruen, 2017). In this computational study, the fluid of interest will be the blood and the biomolecules that can interact in blood. Continuous glucose monitors work as an electrochemical reaction with an enzyme, which oxidizes the glucose and the current proportional to peroxide reacts with platinum for these currents, where the readings are sent to the meter and converted into voltages (Burrin & Price, 1985; Villena Gonzales W, 2019). So, these glucose sensors have different electrodes, including the working, reference, and counter electrodes. The working electrode is coated in the enzyme that will oxidize glucose while the other two aid with holding the voltage and supplying current. Also on the working electrode, the material has to be able to adsorb glucose for sensing. The main focus of this work is finding a proper material for future glucose sensing using knowledge of glucose, the sensing mechanisms, and the properties of the material based on computational properties. This part of glucose sensing research struggles due to excessive costs or low effectiveness of the material, similar to plenty of electrocatalytic reactions, which tend to be a metal or metal alloy. In this case, different Nickel Phosphides are

investigated due to their metallic and nonmetallic properties, with their lower cost and previous successes in other electrocatalytic reactions. However, these nickel phosphides vary in shape and properties based on their metal-to-nonmetal ratio, which was recognized in their results.

2.1.1 Glucose Sensing Mechanisms

When making a glucose sensor, there are multiple reaction pathways potentially involved in the detection process, but there are three main reaction pathways that have been used based on their glucose-sensing abilities. These three include the Glucose Oxidase-Peroxidase method, Glucose Dehydrogenase method, and Hexokinase method (VIVEK N AMBADE, 1998). In the Glucose Oxidase-Peroxidase method, glucose is oxidized to hydrogen peroxide, which was a method stated above. In this method, the H_2O_2 reacts with a chromogen substrate and peroxidase to give a colored product, in which the color intensity represents the glucose present. However, this only works with beta D-glucose, so any alpha D isomers of glucose, which is about 36% of the D glucose, require either more time or the help of the mutarotase enzyme for a higher intensity (VIVEK N AMBADE, 1998). The second method is the Glucose Dehydrogenase method, in which beta D-glucose and NAD^+ react on the glucose dehydrogenase enzyme to form gluconolactone and NADH. The NADH is proportional to the glucose concentration, however, works the same as the Glucose Oxidase-Peroxidase method where time or mutarotase is needed to get the desired results (VIVEK N AMBADE, 1998). The last one, which is arguably the favored one out of the three, is the Hexokinase method. How it works is serum or plasma is deproteinized and glucose reacts with ATP on the hexokinase enzyme and forms glucose-6-phosphate. That, $NADP^+$, and the

glucose-6-phosphate dehydrogenase enzyme form NADPH or NADH, and that is used as the concentration proportional to glucose (VIVEK N AMBADE, 1998). These computational simulations don't focus a specific mechanism but instead on the adsorption of glucose like in chemisorption. In many of these cases, chemisorption would be one of the first steps of the mechanism and thus these calculations are a first step in evaluating the potential of these NiP slabs as glucose sensors. In each mechanism, the glucose or product from the enzymatic reaction will adsorb into a metal slab, such as platinum in the case above, which will have currents that are converted to voltages in the meter.

In glucose sensing research, different bodily fluids have been considered for monitoring glucose efficiently. Currently, the top two bodily fluids include blood and interstitial fluid, which is the fluid that surrounds tissue cells and has similar biomarkers to blood (S. R. Corrie, 2015). Some other bodily fluids include sweat, urine, saliva, breath, and ocular fluid. Blood remains the most widely studied fluid for glucose sensing, with the first and second-generation glucose sensors using blood (Danielle Bruen, 2017; S. R. Corrie, 2015). Both of these original sensing techniques used the Glucose Oxidase sensing method, with the second one being widely known as the "Finger Pricking" technique. This sensor requires the patient to keep track of their glucose levels, especially after potential changes in glucose, including eating and exercise. Some other techniques include the "artificial pancreas" which was introduced in the 1970s as a continuous monitor but not very portable, and the first commercial in vivo monitor, which had the issue of only accessing results every 3 days from a doctor (Albisser et al., 1974; Arvind Jina, 2014; Danielle Bruen, 2017). In the interstitial fluid, a highly studied sensor type is

the use of microneedles as electrodes. This is a patch that penetrates a certain amount to avoid reaching the dermis layer for optimal interstitial fluid sensing. However, this has to avoid sweat and avoid healing of the wound that the patch uses to reach the layer for sensing (Albisser et al., 1974; Danielle Bruen, 2017). This work doesn't necessarily follow a specific bodily fluid, since it is fully computational, however, other biomolecules in the blood that might affect a glucose sensor were studied. Since blood is the most regularly known bodily fluid used in glucose sensing, it makes sense to determine if a potential glucose sensor would work properly in blood. This includes the levels of binding between glucose and these other biomolecules.

2.1.2 Transition Metal Phosphides

Transition metal phosphides are useful catalysts due to their metallic and nonmetallic characteristics, which include stability, conductivity, and catalytic properties. Another beneficial component is the lower cost of these transition metal phosphides, depending on what metals are being used. Other metal/nonmetal alloys have been studied, such as transition metal oxides, selenides, sulfides, TMDCs (transition metal dichalcogenides), and carbon-based materials, but comparatively, transition metal phosphides have better properties (Antara Vaidyanathan, 2021; Seetha Lakshmy, 2023). Compared to phosphides, transition metal oxides tend to be less conductive and less stable, and TMDCs tend to have more toxic properties. This component of glucose sensing requires a catalyst with metallic and ceramic properties, which plays an important factor in determining the ratio of these metal phosphides. In this study, nickel phosphides are used due to nickel's lower cost and catalytic properties. In Laursen et. al, electrocatalysis of the Hydrogen Evolution Reaction (HER) with multiple nickel

phosphides as catalysts and a study with ELF, or the electron localization function through DFT calculations was done (Anders B. Laursen, 2018). This helps determine if the nickel phosphides show more metallic, covalent, or ionic bonding interactions. From 0 to 1, 1 shows a complete localization of electrons, where 0.5 or the midpoint shows an ideal electron gas that's delocalized. In this case, Ni_3P, which is a nickel phosphide that's used in this work, had an ELF of 0.46, which means it was very close to that ideal electron gas, showing both metallic and ionic properties (Anders B. Laursen, 2018). This indicates that this specific nickel phosphide has both metallic and ceramic properties, being useful for stability and catalytic efficiency. Metal phosphides have been used for both oxidation-type reactions and reduction-type reactions, such as OER (Oxygen Evolution Reaction) and HER (Hydrogen Evolution Reaction), and have been efficient in both (Alvarez-Galvan et al., 2019; Seetha Lakshmy, 2023). So, these ideal ELF results could indicate by both Ni_3P's metallic and ceramic properties that it is efficient in glucose sensing since glucose adsorbing into a surface would be an oxidation-type reaction.

Metal phosphides differ by their various structures and their metal-to-phosphide ratios. In this study, more metal-rich nickel phosphides were used due to their higher stability and electronic properties. In Laursen et. al, a study of receiving the cohesive energy and formation enthalpy for determining stability, Ni_3P, Ni_2P, and $Ni_{12}P_5$ as metal-rich nickel phosphides were consistent with their stability, but more phosphorus-rich nickel phosphides less stable (Anders B. Laursen, 2018). For example, NiP_2 was 22% less stable than Ni_2P and the stability started significantly dropping after a Ni/P ratio of 5/4 (Anders B. Laursen, 2018; Seetha Lakshmy, 2023). So, the three nickel phosphides of interest for glucose binding are Ni_3P, $Ni_{12}P_5$, and Ni_2P.

In previous experiments, Ni_2P has been studied in glucose sensing and gave promising results based on sensitivity. In one example, Chen et. al. studied a Ni_2P nanoarray on a carbon cloth for glucose sensing to determine experimental components such as response time, sensitivity, and detection limit (Tao Chen, 2016). To compare the efficiency of the different metal phosphides studied, a review for transition metal glucose sensing compared the different sensitivities, detection limits, response times, etc. Many of the other metal phosphides' sensitivities were below 1000 μA/mM cm^2 while Ni_2P on a carbon cloth was at 7792 μA/mM cm^2 (Seetha Lakshmy, 2023; Tania P. Brito, 2022; Tao Chen, 2016). There were others higher than Ni_2P, including CuO, which is another effective electrocatalyst but oxides tend to be less conductive or less stable (Seetha Lakshmy, 2023), or another nickel-based electrocatalyst. Another nickel phosphide of interest is $Ni_{12}P_5$ since it is a relatively newer metal phosphide, its electrocatalytic abilities, and its Ni/P ratio.

2.2 Proposed Hypothesis

The overall objective is to determine computationally if three different metal-rich nickel phosphides (Ni_2P, Ni_3P, and $Ni_{12}P_5$) are efficient for glucose binding. An important note is that this doesn't necessarily make these slabs glucose "sensors", but rather "binders" since the study is based on their binding. However, the overall binding performances can be used in experimental sensing applications later on (Mingzhu Wang, 2020). To do this, slabs for each of the three NiPs were created using the slab builder tool in Schrodinger (Schrödinger Release 2023-4: Maestro; Schrödinger Release 2023-4: Materials Science Suite) with a glucose molecule placed over the slab in a vacuum-like unit cell. The next step was running the periodic DFT software, Quantum Espresso, in

Schrodinger to determine binding energies and Fermi energies for each slab based on geometry optimizations. The binding energy equation was based on other work that this group has done, (Fujinuma, 2022) and other metal phosphide electrocatalysis (Courtney A. Downes, 2022). The Fermi energy and other calculations were done with Quantum Espresso tools. The equation works by getting the total energies for each component, which includes the slab, the glucose, and the "total reaction" which includes both the slab and glucose. This equation ensures that everything in this unit cell is accounted for, and the more negative the binding energy is, the stronger the bind is. The binding energy equation is below:

$$Binding\ Energy\ (BE) = E_{Total(Slab+Glu)} - \left(E_{Total(Slab)} + E_{Total(Glu)}\right) \qquad (1)$$

The slab requires full optimization before the reaction proceeds and when optimizing both the glucose and the slab, the slab must be as frozen as it can be. The Fermi energy was used to determine a better transfer of electrons from the glucose to the slab. So, in this case, a less negative value corresponds to a better transfer of electrons. Density of States (DOS), Projected DOS, and BAND structures were also used to determine the properties of the slabs. Fermi levels were given in the DOS.

2.2.1 Metal-Rich Nickel Phosphides

As stated above, P-rich Nickel Phosphides aren't used because of their lower stability due to their weaker P-P covalent bonding. Since metal-rich nickel phosphides have more ionic and metallic bonding, they are more efficient in glucose sensing. For glucose sensing, there are three main points to have the most desired glucose sensor that are followed in this work. Those are high conductivity, more active sites, and easily

accessible for glucose (Seetha Lakshmy, 2023). With more metallic and ionic bonding, metal-rich NiPs are more conductive. Metal phosphides form more amorphous structures rather than layered structures that sulfides would form, so that makes the slab have more active sites due to having corners and edges accessible. The structures of metal-rich NiPs form triangular prisms as the smallest possible structure and any other metal atoms will result in forming ninefold tetrakaidekahedral coordination (Alvarez-Galvan et al., 2019). The overall goal of this section is to determine which metal-rich Nickel Phosphide will be the most effective binder and compare them to their Ni/P ratio, accessibility, active sites, conductivity, and previous electrocatalytic knowledge of them, as a potential glucose sensor by binding. In a future outlook, this can help determine what Nickel Phosphide would be useful in a glucose sensing approach, in an experimental study for example.

2.2.2 Glucose Binding in Blood VS Other Biomolecules

Another important concept in glucose sensing is how effectively the sensor works compared to other biomolecules that may come in contact with the sensor. In this case, how effective glucose binds VS other biomolecules. Blood biomolecules were used since blood is the most significant bodily fluid for glucose sensing. The biomolecules chosen were based on a previous experimental Ni_2P glucose sensing work, which was mentioned above. Chen et. al. used five different biomolecules that are significant in blood experimentally and determined that there were no significant responses with these biomolecules over glucose on Ni_2P (Tao Chen, 2016). So, would that still be the case on all three slabs, including comparing the data to Ni_2P computationally? From this work, four out of the five biomolecules were tested over the three slabs to determine if the biomolecules would perform the same on Ni_2P and how they would work over the other

two. The four biomolecules used were Fructose, Ascorbic Acid, Dopamine, and Uric Acid. Fructose was run over all three of the slabs while the others were only run on the leading slab, which ended up being Ni_3P. The reason for running fructose over all three was because glucose and fructose have similar electroactive behaviors (Tao Chen, 2016). For that same reason, lactose was ignored from that work since it also has similar electroactive behaviors as glucose and fructose (Tao Chen, 2016). The other three were only run on Ni_3P because it was expected that the slab would be the most effective out of the three, and it wouldn't make much sense to perform extra work over Ni_2P, which has been done in Chen et. al., and $Ni_{12}P_5$ was the least effective out of the three so that was ignored.

2.2.3 Computational Methods

For all of the glucose binding work, features in both the Materials and Maestro GUIs in the Schrodinger software were used (Schrödinger Release 2023-4: Maestro; Schrödinger Release 2023-4: Materials Science Suite). To create these slabs, the Slabs and Interfaces tool in Schrodinger was used, which gave access to configuring the Miller Indices, the size of the slab, and the space needed in the vacuum-like unit cell. Miller Indices are planes that correspond with a 3D axis, in an *hkl* notation, with the axes referring to *abc* (Hendrik J.R. Lemmer, 2022). The most common notation of Miller Indices refers to a (0,0,1) formation, however, this work consisted of Miller Indices that fit a glucose molecule properly and had enough space to be a vacuum cell. The vacuum cell had around twenty more angstroms of space, which allowed movement and no forced interaction of the glucose to the slabs. The three NiPs done were Ni_3P, Ni_2P, and $Ni_{12}P_5$. The Miller Indices for each of the three respective NiPs were (0,0,1) (Liangcai Zhou,

2010), (2,2,1) (Daisuke Kanama, 2004), and (0,0,1) (Jain et al., 2013; Zhiqun Ran, 2021) and they each had a similar number of atoms, being 32, 36, and 34 atoms.

With these slabs, a glucose molecule was placed over the slab and run in the Quantum Espresso software that is also included in Schrodinger (Giannozzi P, 2017; Paolo Giannozzi, 2009). In Quantum Espresso, these calculations were DFT minimum energy geometry optimizations using the PBE (Perdew, Burke, and Ernzerhof) functional (John P. Perdew, 1996) with a convergence threshold of $1*10^{-6}$ Ry, or $5*10^{-7}$ Hartrees. The slabs were frozen to the best of their ability while running. In these calculations, gamma points (Γ) were included, which is the center of the Brillouin Zone. The Brillouin Zone in solid-state chemistry and physics represents vectors perpendicular to the Miller Indices bisectors (Harald Ibach 2009). The Brillouin Zone is related to the K points, representing the whole unit cell rather than just the space (Peter Kratzer, 2019). The set of K points in these calculations was the Monhorst and Pack grids, which were 3x3x1 in all these simulations. The simplest "periodic" system is made up of one K point, which would also be the Γ point (Hassan, 2015). These calculations also included Quantum Espresso components such as PDOS, DOS, BAND structures, phonons, and charge density surface to give those three graphs, including free energies and Fermi energies (E. Bekaert, 2008). That can give information such as free energies, transfer of electrons, and bandgap. The DOS/PDOS plots gave information about overlapping bandgaps that metals have with information on energy levels. The BAND structure is used to compare to the DOS data and the levels of activity in either the conductance or valence bands. Both the Fermi levels and energies were obtained from these components. Any other components were deemed insignificant for determining efficiency as a glucose sensor. With those

results, “single point energy” type calculations were done in Quantum Espresso, with no components added and everything frozen to get the total energies of the total reaction, the slab, and glucose to get binding energies in equation 1. The binding energies resulting in the more negative is better binding. Fermi energies were determined as the most electron transfer by the least negative value in eV. The Fermi Level represents the work needed to move an electron either to or from the material studied (Kahn, 2016), which confirms a favored transfer of electrons with a lower negative value. In this work, Fermi energies and levels represent the same value, but that is not always the case. It all depends on the temperature. The Fermi Level represents the energy at absolute zero and energy can be represented at any temperature (Kahn, 2016). Both Fermi energies and levels were found through the DOS and the energy property, which gave the same values. The DOS/BAND values were also plotted “zero to Fermi energy” which just sets the zero energy level on the horizontal axis to the Fermi energy instead. The Integrated DOS was also added to the DOS plot, with the right side vertical axis showing that. For the other biomolecules VS glucose, the biomolecules only had binding energy calculations done, which was significant enough to compare binding and determine which bound was the strongest.

2.3 Computational Results

All three of the Nickel Phosphides showed affinity towards interaction with the glucose, and even binding in some of the cases, which was the first step in the glucose sensor process. The second one was determining the effectiveness of binding based on their binding energies and Fermi energies in this case. Based on their structures and their previous electrocatalytic or glucose sensing works, these simulations should all have negative Fermi energies and binding energies, which they did in Table 2.1. These binding

energies were calculated with Equation 1, consisting of three different single-point energy type calculations to determine each factor in the equation. This binding energy represents the energy between structures that shows interaction or binding, which is always negative. With no binding whatsoever, the binding energy would be zero, or just remain the same as their single-point energies with more negative binding energies corresponding a stronger binding between the slab and molecule. The Fermi energy represents the space between the valence band and conduction band of the electron energy, while metals tend to overlap in those cases. Nonetheless, this energy still represents the energy difference between the highest and lowest occupied orbitals between the two systems (Harald Ibach 2009). The negative values can indicate an interaction between electrons with a lesser negative indicating more transfer (Tarr, 1999). The ratios of nickel to phosphide were also done to determine if a higher Ni content would properly compare to the glucose sensing abilities. The leading slab in binding performance was Ni_3P in this case, with the most negative binding energy and least negative Fermi energy while the least favorable Ni_xP_y compound was $Ni_{12}P_5$. Density of States (DOS) plots were done and confirmed that these three were all metals and had metallic characteristics.

With the binding energies of fructose, it was also determined that fructose binding was unfavorable compared to glucose in most cases. However, fructose binding was more favored on $Ni_{12}P_5$ than glucose, which is concerning if the slab is used in experimental glucose sensing. Ni_3P is still the leading slab out of the three, while Ni_2P had the weakest interaction with fructose.

Table 2.1

Nickel Phosphides Studied and Compared by Their Nickel-To-Phosphorus Ratio

Nickel Phosphide	**Binding Energy (eV) of Glucose**	**Fermi Energy (eV) of Glucose**	**Binding Energy (eV) of Fructose**	**Ni/P Ratio**
Ni_2P	-0.671781092	-0.930112386	-0.030122936	2
$Ni_{12}P_5$	-0.345856716	-1.434869991	-0.860707802	2.4
Ni_3P	-0.848655102	-0.849430626	-0.088749735	3

2.3.1 $Ni_{12}P_5$

Being a lesser-known Nickel Phosphide, there was plenty of interest in how this one would work. There have been multiple electrocatalytic reactions studied for this slab (Chunde Wang, 2015), but nothing done in terms of glucose sensing. Since more metal-rich metal/nonmetal alloys have been of interest for glucose sensing, this nickel phosphide was chosen because of its high Ni/P ratio. The structure, shown in the middle of Figure 2.1, has some interaction between the glucose and slab, but no specific binding. That's sufficient because the vacuum-like unit cell with plenty of extra space means it wasn't forcing interaction between the two. This slab was the least favorable based on

binding performance, having the least negative binding energy and the most negative Fermi energy. The binding energy was -0.356 eV, and the Fermi energy was -1.435 eV. This slab was the only slab that was towards the middle of the unit cell rather than the bottom. That, however, doesn't effect the results since these would be a repeated series on all three axes, resulting in an equal space between all other unit cells near this cell. Some potential reasons why this slab gave poor results could be due to its structure and properties being lesser known compared to the other two. Also compared to the other two, this was the only slab that didn't bind to the surface while the others did. The visual structure can help confirm that this slab was unfavorable with no binding to the surface.

This slab gave unexpected results with fructose interactions since the fructose preferred binding to the surface over glucose. The structure is located below, in the middle of Figure 2.2, which shows visually that fructose is bound to it. However, in Figure 2.1, there is no binding of $Ni_{12}P_5$ to glucose. A potential reason for this was forced interaction of the unit cell, but there is the same distance in both unit cells, so that does indicate the preferred binding of fructose.

2.3.2 Ni_2P

This slab was employed in previous glucose sensing experiments. In these experiments, Ni_2P has shown high sensitivity for glucose in multiple sensor designs (Seetha Lakshmy, 2023; Tao Chen, 2016) and has been useful in other electrocatalytic reactions (Shu Fujita, 2020). However, there weren't any details on computational work with Ni_2P but this slab was used as a baseline calculation for the other two since there has been some experimental work done on it (Tao Chen, 2016). This one was expected to be

either the most desirable or the second. Looking at the nickel-to-phosphorus ratio, assuming that the ratio would be important to the glucose sensing abilities, this would have the least negative binding energy and most negative Fermi energy. However, this one was in the middle of the three slabs with a binding energy of -0.67 eV and a Fermi energy of -0.93 eV. This structure, shown on the left of Figure 2.1, is physically bound to the structure which could also be a visual representation of glucose binding to the slab. As stated before, these slabs are made up of multiple unit cells next to each other in all different axes, so there are two atoms on the top of the slab, which just indicates that is part of the cell above. The one below this slab would also include those two atoms, which would also be a part of this slab. This can happen when the slab isn't fully frozen, which did happen throughout the geometry optimizations. However, the structure still gave proper energies to compare to. A difference in this slab between the other two was the Miller Indices being (2, 2, 1) instead of (0, 0, 1) because the size of the slab from the original structure file was a lot smaller than the other two. That doesn't have influence, since the goal was to keep the structures a size big enough to fit a glucose molecule in the unit cell and to interact.

The fructose and Ni_2P structures are located on the left of Figure 2.2, and it had the weakest binding to fructose in Table 2.1. The binding energy, being -0.030 eV, shows very weak interactions, which lines up with the previous experimental work, stating there was little or no change in response to the addition of fructose over glucose (Tao Chen, 2016).

2.3.3 Ni_3P

Out of the three slabs, this one had the strongest binding energy. Originally, it was thought to have inadequate results, due to its catalytic abilities in the HER reaction, since more phosphorus-rich metal phosphides are more prominent in those reactions. Another thought was that where is the point where the ratio of metal to phosphorus is too high where more metal would be detrimental, since Ni_3P has a 3 to 1 metal ratio. However, it was the most favored with both the binding energy and Fermi energy being around -0.85 eV. The structure on the right of Figure 2.1 also shows binding, just as in the Ni_2P structure. The glucose molecule is flat rather than sideways, which could mean stronger interaction. On the side could be interpreted as it had to be sideways to bind, showing less interaction and active sites compared to this structure. More details are listed below in the discussion on why it could have been the most desirable. These include the ELF value and a slight bandgap in the DOS graph.

With fructose added instead of glucose, the structure below on the right of Figure 2.2, there was very little interaction at all based on the visual structure and energies, similar to Ni_2P. The binding energy is slightly larger, but not large enough to be significant. This was the leading slab with glucose, so the other three biomolecules were done on top of this slab only. Since the interaction over glucose was the strongest and the interaction over fructose was weak, the other three being weak would be a great sign for Ni_3P.

Figure 2.1

The Fully Optimized Structures of (a) Ni_2P, (b) $Ni_{12}P_5$, and (c) Ni_3P With Glucose

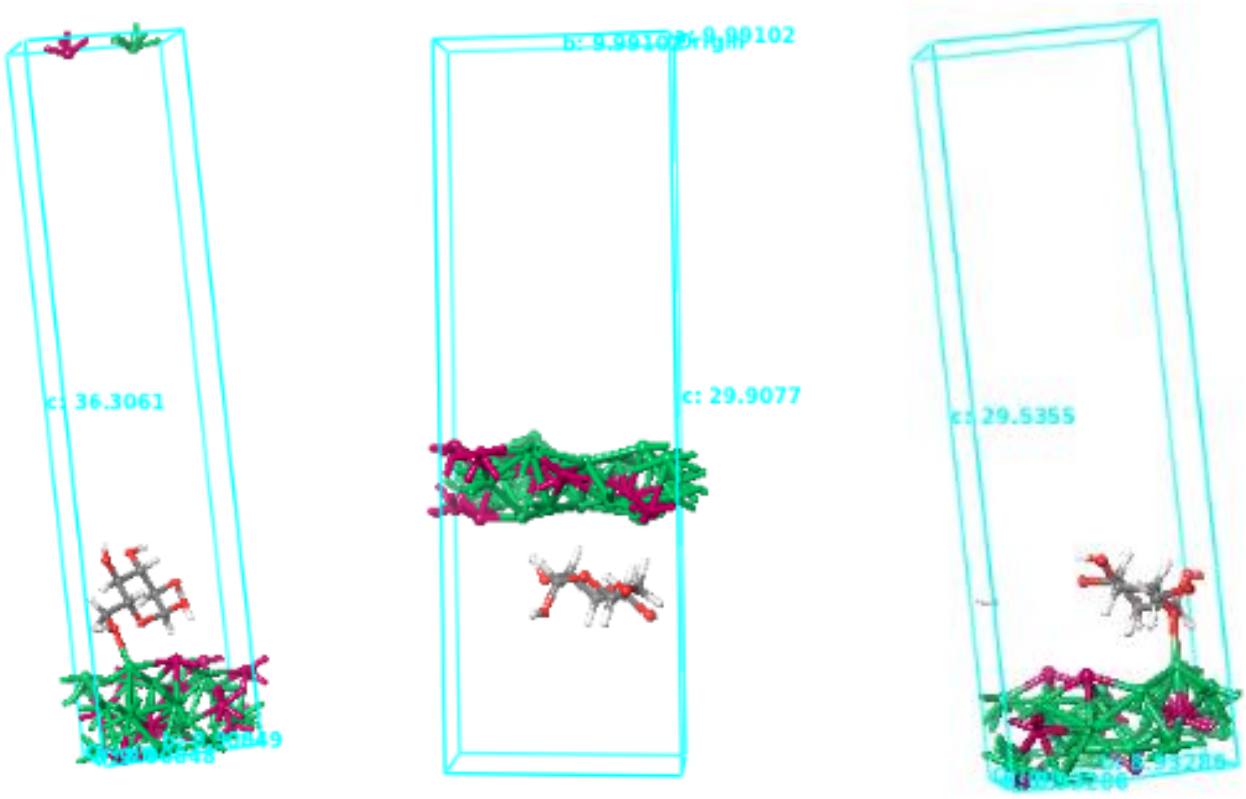

(a) Ni_2P (b) $Ni_{12}P_5$ (c) Ni_3P

Figure 2.2

The Fully Optimized Structures of (a) Ni_2P, (b) $Ni_{12}P_5$, and (c) Ni_3P With Fructose

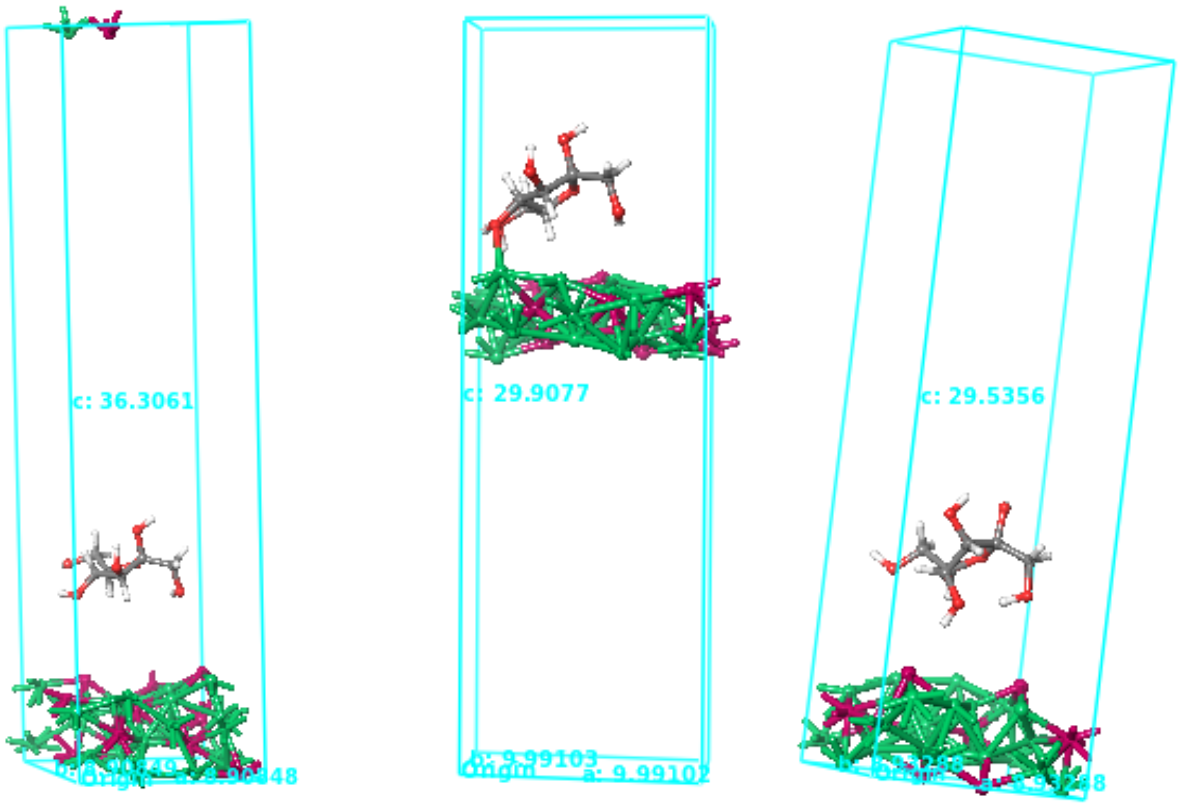

(a) Ni_2P (b) $Ni_{12}P_5$ (c) Ni_3P

As stated above, the DOS data had no bandgap between all three slabs' plots, labeling them as metals. The way that was determined was in Figure 2.3 below, there was a nonzero value for the density of states at the energy level of zero. Something like a semiconductor or insulator would have a clear indication of zero states (Kahn, 2016). Based on the PDOS data, it was determined which peaks belonged to which electron states which also confirms the metallic behavior. The charts aren't included since there was no energy shift or higher peaks involved. The peak in the -100 eV range represents the 3s orbital, the peak in the -60 eV range represents the 3p orbital, and the big peak in the 0 eV range represents the 3d orbital for all three graphs. All the little peaks from 0 to -20 eV represent all the other shells and subshells between all three graphs. This makes sense with Ni's electron configuration, filling up the 4s subshell and partially filling up the 3d subshell. Both the 3d and 4s subshells are represented near the zero mark, indicating the difference between the valence and conduction bands (Liangcai Zhou, 2010). Since metals have an overlap between the two bands, this makes sense and confirms that all three slabs are metallic. Lastly, the Integrated DOS was done in the dashed lines of the DOS. This line represents the integrated number of energy levels (S. Jelev-Vlaev, 2009). This also makes sense because the energy levels increase as more and more energy levels are also represented by the PDOS. Since most of the energy levels are located in the peaks around 0 eV, the integrated DOS grows quickly.

The BAND structures are also included for the three slabs, indicating that most of the energies are negative, meaning they are more involved with the valence band of the DOS (Kahn, 2016). These are located in Figure 2.5. With previous PDOS/DOS data of Ni_3P especially, that makes sense (Liangcai Zhou, 2010). The Fermi Levels of all three

slabs reside in that valence band, which also makes sense since that lies in a more active region (Kahn, 2016). The more activity going on in both the DOS and BAND represents more electronic activity = more active. In the DOS plots, the majority of the peaks are contained in the negative regions.

The DOS plots of just the slabs were done to determine if there was any shift or any difference in states between the with and without glucose DOS plots. The slab-only DOS plots are located in Figure 2.4. Overall, there was no shift, and the states remained the same, with the -100 eV peak being the 3s orbital, the -60 eV peak being the 3p orbital, and the big peak at 0 eV being the 3d orbital. The 4s orbital was also located around the 0 eV area, but at a smaller peak also indicating the difference between the conduction and valence bands. There was also less noise from 0 to -20 eV, which also makes sense due to the lack of glucose. The Fermi energies were bigger, which makes sense due to the lack of electron transfer and more electrons overall on the slab. These Fermi energies for Ni_2P, $Ni_{12}P_5$, and Ni_3P are -1.546 eV, -1.887 eV, and -1.579 eV.

Figure 2.3

The Density of States (DOS) Plots for Glucose and (a) Ni_2P, (b) $Ni_{12}P_5$, and (c) Ni_3P

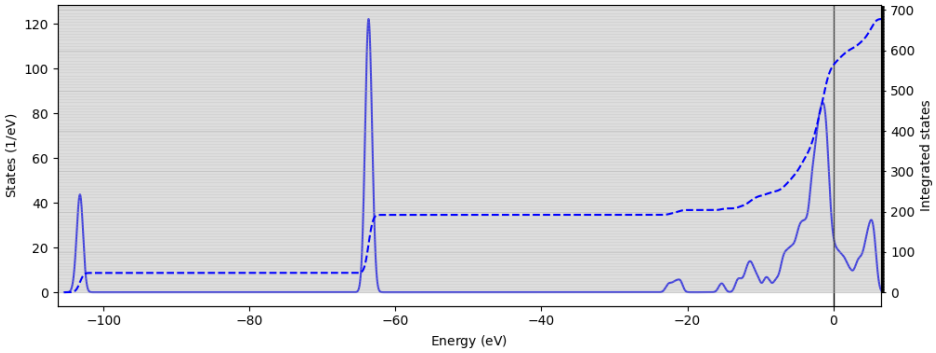

(a) Ni_2P + Glucose

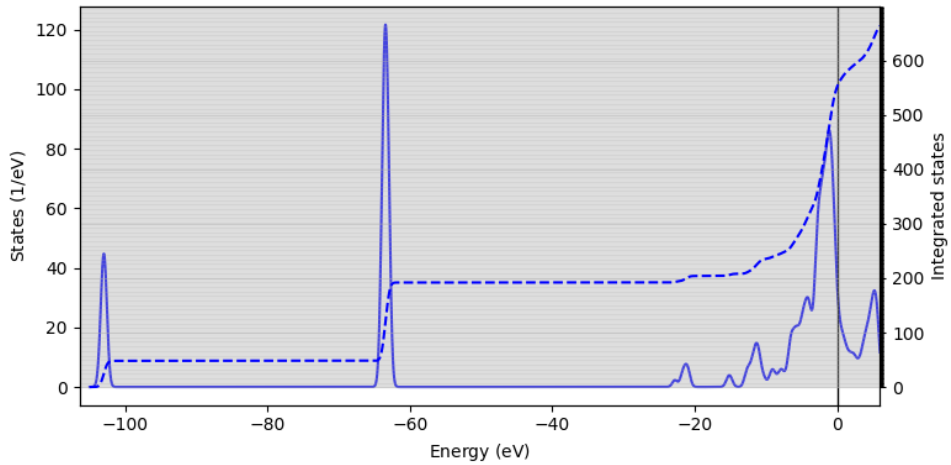

(b) $Ni_{12}P_5$ + Glucose

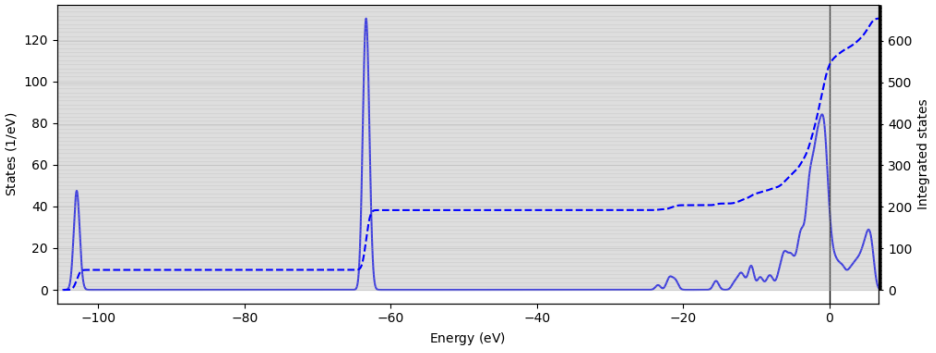

(c) Ni_3P + Glucose

Note. The dashed lines represent the integrated DOS, and the solid line represents the DOS.

Figure 2.4

The Density of States (DOS) Plots for Just the Slabs of (a) Ni_2P, (b) $Ni_{12}P_5$, and (c) Ni_3P

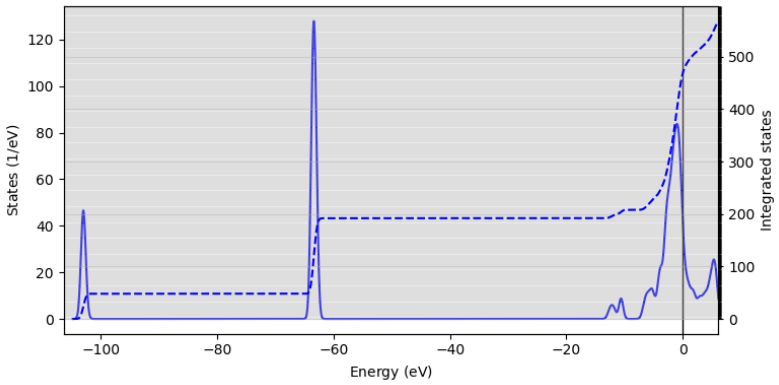

(a) Ni_2P Slab

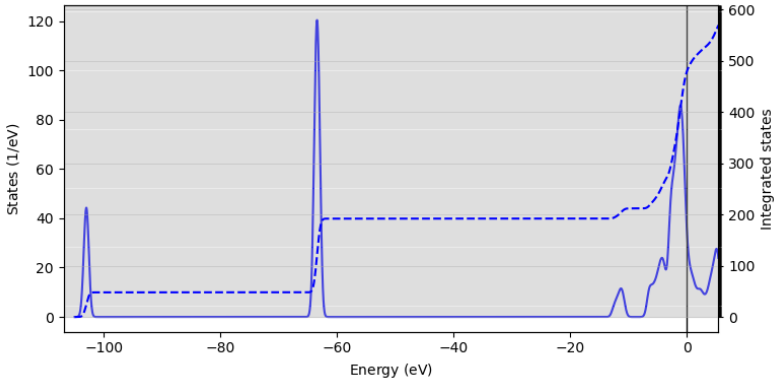

(b) $Ni_{12}P_5$ Slab

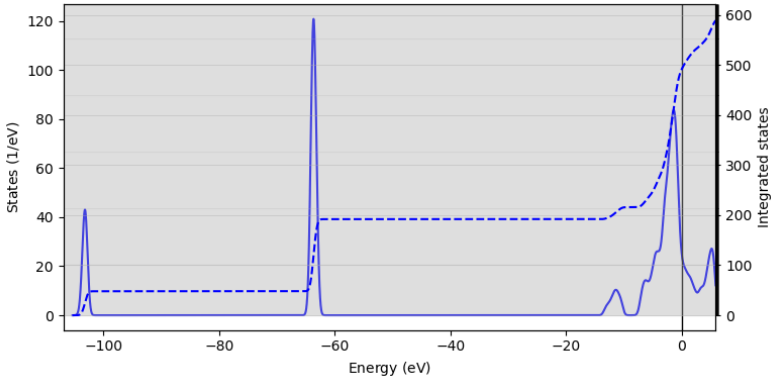

(c) Ni_3P Slab

Note. The dashed lines represent the integrated DOS, and the solid line represents the DOS.

Figure 2.5

The BAND Structures of (a) Ni_2P, (b) $Ni_{12}P_5$, and (c) Ni_3P + Glucose

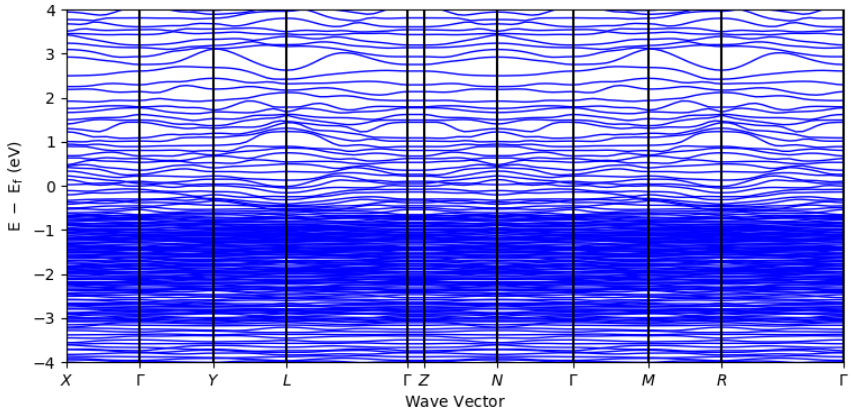

(a) Ni_2P

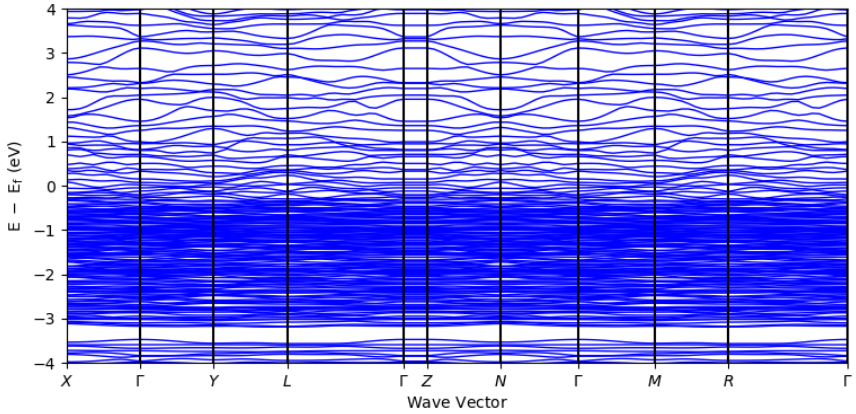

(b) $Ni_{12}P_5$

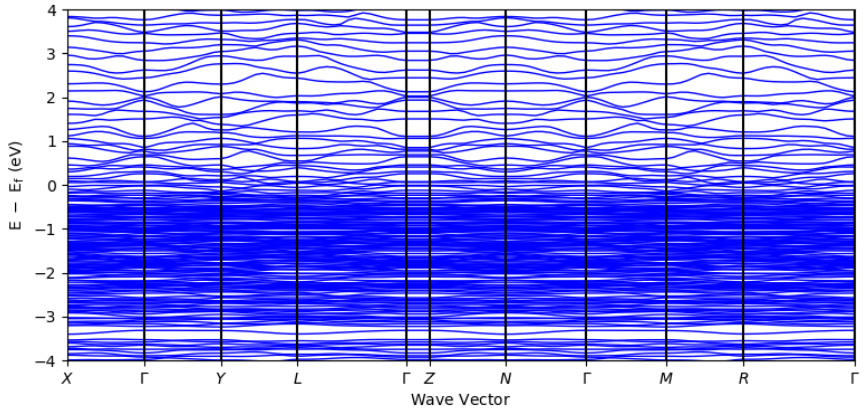

(c) Ni_3P

2.3.4 Glucose Binding in Blood VS Other Biomolecules

In Table 2.2, all four biomolecules done over Ni_3P including glucose are shown. Overall, glucose was the preferred biomolecule as far as binding to the surface of the slab with no close second. One important note is that the structures below, in Figure 2.6, of Dopamine, Ascorbic Acid, and Uric Acid have no indication of bonding and their binding energies are very low. The closest to glucose was fructose, which still doesn't have any significant binding based on the binding energy. This proves that in blood, Ni_3P can work well as a glucose-binding tool.

Table 2.2

Binding Energies (in eV) on Ni_3P of Glucose VS the Other Biomolecules in Blood

Biomolecules	**Binding Energies (eV)**
Glucose	-0.848655102
Fructose	-0.088749735
Dopamine	-0.018217982
Uric Acid	-0.00699331
Ascorbic Acid	-0.04406874

Figure 2.6

The Fully Optimized Structures of Ni_3P with (a) Dopamine, (b) Ascorbic Acid, and (c) Uric Acid

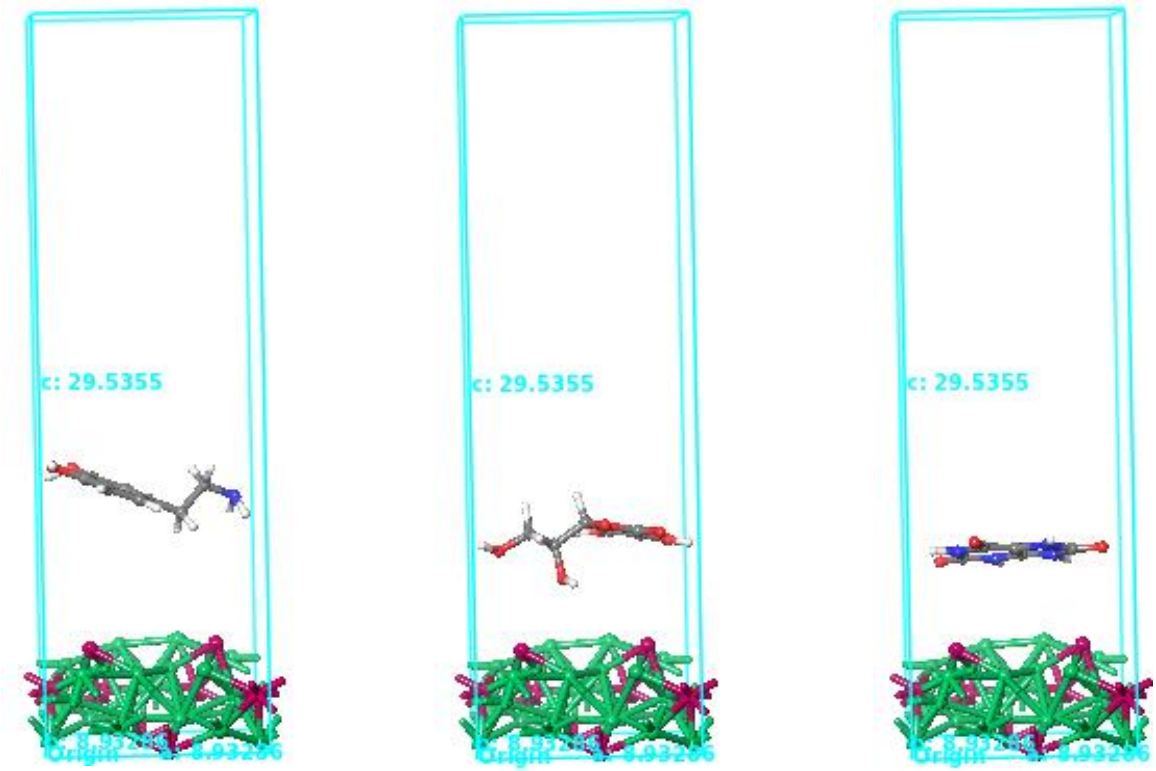

(a) Dopamine (b) Ascorbic Acid (c) Uric Acid

2.4 Discussion

When calculating the binding energies and Fermi energies, it is important to note that there were no discrepancies between the more negative binding energies and the less negative Fermi energies. For example, Ni_3P was the leading slab by having the most negative binding energy and the least negative Fermi energy rather than a different standing, and the same works for the other two slabs. There were no issues with one having the strongest binding energy but not the most favored Fermi energy for example. This means that the binding energy and the transfer of electrons are correlated, meaning that the slab can transfer electrons more easily, making it easier to bind. Other glucose sensing properties such as active sites, metallic properties, and catalytic properties can influence these components additionally.

2.4.1 Performance of Sensor VS Ni/P Ratio

Out of the three slabs, there was no specific trend for the performance of the sensor versus the Ni/P ratio. The outlier, in this case, is $Ni_{12}P_5$ since the sensor abilities increase from Ni_2P to Ni_3P. Because this slab was the outlier, $Ni_{12}P_5$ was looked at more to determine any anomalous properties. Zhang et al. did extensive studies on the properties of Ni_2P and $Ni_{12}P_5$ and determined that Ni_2P had more favored properties such as absorption rate and light absorption capacity (Dong Zhang, 2021). In addition to that, $Ni_{12}P_5$ had weaker bonds due to 3p states being more delocalized and microagglomeration (Dong Zhang, 2021). A proposed hypothesis for why $Ni_{12}P_5$ was deficient is due to its structure and more localized states. Ni_2P was used as a baseline calculation, which gives information that Ni_3P could be a desired sensor, even when Ni_2P

had high sensitivity on a carbon cloth and graphene (Seetha Lakshmy, 2023; Tao Chen, 2016). It doesn't necessarily mean that $Ni_{12}P_5$ would be a poor sensor, it just means on its own it's the least effective sensor compared to the other two. However, fructose data indicates that it would be insignificant to study it more. The same goes for Ni_3P, where its performance can vary in an experimental application. However, it was the most favorable on its own in this computational study. A trend that was of interest was based on the stability and conductivity levels of the metal-rich slabs. As stated above, Laursen et. Al has stated that stability is consistent with the metal-rich slabs but starts to drop when the Ni/P ratio becomes 5/4 (Anders B. Laursen, 2018). In this case, the lowest Ni/P ratio was 2/1 so that was not as much of a concern. For glucose sensing, conductivity, active sites, and high accessibility were the three main factors when creating a sensor. All three structures seem to interact with Ni on the surface visually, whether they are bound to the structure or not. However, binding is what indicates which sensor is the most desirable for future studies. That would put Ni_2P and Ni_3P over $Ni_{12}P_5$. $Ni_{12}P_5$ is bound to the surface in fructose only, which also puts the other two ahead for glucose sensing. Another indication would be how the glucose bound itself to the surface. The Ni_2P structure having the glucose bind sideways could indicate that there are fewer active sites, and the glucose could only bind to one specific site rather than having other options. The Ni_3P structure being flat can indicate that there are other binding sites, and no electron-electron repulsion caused it to go perpendicular to the slab. This makes sense, with previous work indicating that Ni_3P with both Ni and P on the surface also has a reactant interact with the P (Liangcai Zhou, 2010). With fewer active sites, there would be a lower accessibility for glucose due to fewer places to bind or interact with the slab. In these slabs, it was

expected to see more interactions over nickel rather than phosphorus since these are metal-rich slabs. So, in that case, more metal-rich slabs such as Ni_3P would be preferred over the other two. These metal-rich slabs have more ionic bonding, and ionic bonds are stronger than covalent bonds.

Between the three slabs, the Miller Indices vary, with both Ni_3P and $Ni_{12}P_5$ having a (0, 0, 1) formation and Ni_2P having a (2, 2, 1) formation. This was done to properly fit a glucose molecule over the slab in the unit cell. A concern was whether that would cause issues based on the number of active sites or interactions with nickel since other studies have used (0, 0, 1) for Ni_2P. However, Zhang et. Al had a similar surface as this work, with both Ni and P on the surface when conducting their experimental studies so this was disregarded (Dong Zhang, 2021).

2.4.2 Ni_3P as the Favored Slab

Ni_3P had the most desirable results as a glucose sensor, with both Fermi energies and binding energies around -0.85 eV. As stated before, it was first hypothesized to be the least effective glucose sensor due to its HER catalytic abilities. According to Laursen et al., its catalytic abilities were comparable to Ni_5P_4 and other phosphorus-rich nanoparticles for HER catalysis (Anders B. Laursen, 2018). However, based on its ELF value from the same work, it can be used for both oxidation and reduction reactions for electrocatalysis. The ELF value states that around 0.5, the midpoint, the electrons are delocalized and act like an ideal electron gas. With Laursen et al. having an ELF of 0.46, it is close to that ideal electron gas (Anders B. Laursen, 2018). That can indicate that with both metallic and ceramic properties, Ni_3P can be useful in both a metal-rich and

phosphorus-rich Nickel Phosphide electrocatalytic reaction. That can indicate how Ni_3P was efficient in both glucose sensing, which is this work, also HER electrocatalysis. However, there were no details on the ELF values for either Ni_2P or $Ni_{12}P_5$. Based on this work's data and other electrocatalytic work, those two slabs are most likely more metallic rather than a mix of metallic and ceramic properties.

Another interesting point to make is that in the DOS plots, both the Fermi Level and any potential bandgap were given in Schrodinger. Ni_2P and $Ni_{12}P_5$ had no bandgap and were simply listed as "metal" while Ni_3P had a very small bandgap of 0.028 eV in the glucose + slab plot. There is no visual representation in either Figures 2.3, 2.4, or 2.5 showing that because it's so small, but that could play a factor in its efficiency. The BAND details listed the same Fermi Level and bandgap but listed Ni_3P as "metal" in that case with the other two. This small bandgap was interesting though, because this could suggest that Ni_3P did have slightly different properties than the other two slabs, with some semiconducting properties. An important note is that ceramic properties from the phosphorus do not indicate semiconducting properties, it is just important in the catalytic efficiency. However, previous works on Ni_3P suggested that this is not the case. Ni_3P exhibits strictly metallic characteristics but is useful as a catalyst based on active Ni-P bonds (Liangcai Zhou, 2010). The slab-only plot for Ni_3P also had no bandgap or shift from the glucose + slab plot, which also indicates that it is metallic. The thought process of why that would be the case was the potential moving of the original Ni_3P slab since there was trouble freezing these slabs fully when the reaction happened on it. The reason why this small bandgap was disregarded is because of knowing the characteristics of Ni_3P which are similar to the other two and seeing that it was listed as "metal" in the

BAND data. This was interesting to see, however. The way that could affect this is by shifting the energy slightly and giving this bandgap. There was no sign of shifting in the PDOS, but this still could be due to an energy change between the before and after products.

Among the other biomolecules, Ni_3P also had the most negative binding energy for glucose by a significant amount. That indicates that glucose would bind to Ni_3P over any other biomolecules. In a glucose sensing application, glucose should bind strongly to the surface rather than another biomolecule. In this case, Ni_3P binds ten times stronger to glucose than fructose, and fructose is the second most effective binder. Compared to $Ni_{12}P_5$, fructose was favored over glucose on that surface, which means it wouldn't be as good of a glucose sensor. The structures of fructose compared to glucose were considered for this particular case, since they're isomers and both monosaccharides but had completely different properties. So, an interesting structural feature was that glucose is an aldehyde and fructose is a ketone. This can play a factor because aldehydes tend to be more reactive and have hydrogen bonded to the central carbon that's also bound to the oxygen of interest, rather than two different chains. This hydrogen can potentially leave more room for oxidation, which can lead to more reactivity. Plenty of the glucose sensing mechanisms result in oxidation, which would benefit the binding of glucose over fructose.

Another important factor to consider is if the binding of glucose is too strong to be an effective glucose sensor. The strong binding can be detrimental due to no transfer to a product and in an experimental glucose sensor, glucose produces a product and a byproduct which is proportional to the glucose concentration and is the way to detect the

amount of blood glucose in the blood. However, in these computational simulations, the Fermi energies are used to determine that there is still a relevant charge transfer between the three slabs, and a reaction can potentially still be done.

Chapter 3

Electrocatalysis of CO_2 to DMC on an Au/Pd Alloy Slab

3.1 Introduction

3.1.1 Electrocatalysis in an Environmental Perspective

Electrocatalysis is used in plenty of environmental applications, such as HER, OER, ORR, water splitting, and the focus of this section, CO_2 reduction. CO_2 in the atmosphere has been an issue from global warming, including other greenhouse gases. Overall, CO_2 contributes around 79% of greenhouse gases as of 2021 with a majority being produced by transportation, electricity, and industry (Masson-Delmotte, 2021). Plants consume CO_2 regularly, but these levels of emission cannot be consumed by only plants. An overall objective would be to produce a catalytic resource to reduce or capture CO_2. Just like the glucose sensing applications above, the overall goal is to speed up a reaction with a catalyst or make said reaction more spontaneous. Reactions like HER or CO_2 reduction struggle to reach a larger scale application due to a bunch of factors such as cost and catalytic abilities (Shulin Zhao & Chen, 2019). Similar to glucose sensing above, metals and metal alloys are common catalysts in these reactions. These metals include transition metals, MOFs (metal-organic frameworks), and metal/nonmetal alloys such as TMOs, TMPs, TM sulfides, and selenides (Tran Thanh Tam Toan, 2023). In this study, a gold/palladium alloy is studied as an electrocatalyst for CO_2 reduction. In this application, the overall goal is to reduce CO_2 to a more useful compound on the metal alloy computationally rather than as a greenhouse gas in the atmosphere.

3.1.2 Metals, Bimetal Alloys, and Metal/Nonmetal Alloys

In electrocatalysis and other metal-based chemistry, metals have been known to be great catalysts based on their metallic properties. However, metals can only provide certain properties based on the metal and can end up being less efficient than metal alloys or metal/nonmetal alloys. On their own, metals can have different catalytic abilities and structures based on size. For example, smaller Au NPs (nanoparticles) tend to be disordered and have great catalytic abilities at many different temperatures while larger ones have a more ordered structure that doesn't perform as efficiently at lower temperatures (Yang Hea, 2018). However, metal alloy nanoparticles are more desirable than single metal nanoparticles because they can restructure dynamically under specific reactive states. That's because of different binding strengths that are contributed by the metallic components and the adsorbate that's reacting with the alloy (Mengyao Ouyang, 2021). These active sites changing in the gas phase can help create and control reaction surfaces in catalytic reactions. In Ouyang et al, both temperature conditions resulted in Pd aggregating to the surface before CO was introduced, which resulted in stronger binding with Pd on the surface (Mengyao Ouyang, 2021). An example like that can show how the use of Pd can create a more reactive surface with stronger binding in the case of CO catalysis.

Other metals, such as Nickel, can absorb well and contain properties that other catalytic metals have, however, metal alloys can benefit from the properties of multiple metals, or even other nonmetals if the alloy has both (Seetha Lakshmy, 2023). An example using nickel states that pure nickel catalysts are used in alkaline electrolyzers but have low activity and dissolve in acidic conditions (Anders B. Laursen, 2018). That

work is referenced for the glucose sensing section of this thesis, which used Ni_3P for HER electrocatalysis and showed efficiency in both alkali and acidic conditions. In that case, the ceramic properties of phosphorus aided its catalytic abilities in addition to the conditions in which electrocatalysis can happen. This is a great example since nonmetals can help aid the catalysis of a metal by providing ceramic properties, ionic bonding, covalent bonding, and more active sites to a structure to increase reactivity, stability, and other properties that are necessary for a great catalyst.

In this section, an electrocatalytic reaction of CO_2 reduction is done on an Au/Pd slab. The overall goal is to reduce CO or CO_2 to some useful compound that can be used in a laboratory or other settings. That can help reduce CO_2 in the atmosphere and recycle it into something useful on a large scale. This reaction consists of three different slabs: a Pd slab, an Au slab, and a 50/50 mixture of the two metal alloys. The overall goals were to determine which slab was the most efficient, which product was preferred, the mechanism of the reaction computationally, and compare it to the experimental work done. The two potential products consist of DMC (dimethyl carbonate) and DMO (dimethyl oxalate).

3.2 Proposed Hypothesis

3.2.1 Proposed Mechanisms

In this section, the overall hypothesis is to prepare slabs of different amounts of Au and Pd to determine a mechanism for the CO-to-DMC reaction. To do this, four-layered slabs were created with two pure metal slabs of Au and Pd, including a 1-to-1 ratio of Au and Pd on a “checkerboard” slab. It was called a “checkerboard” slab because

the metal atoms were separated into four different regions to match the experimental work, which had different "bands" of each metal rather than a homogenous mixture (Fujinuma, 2022). These slabs were created in the AMS (Amsterdam Modelling Suite) (R. Rüger, 2023) slab builder tools and first optimized using DFTB. With the optimized slabs, they followed the reaction:

$$CO + 2CH_3OH \rightarrow DMC \quad (2)$$

By freezing the fully optimized slabs and running this reaction with the same method as the slab optimizations, with one intermediate and two transition states in between. The overall experimental reaction consists of three separate steps, but this was the reaction followed in a computational setting. These transition states were done by running 2D reaction coordinate scans along the O-H and C-O bonds to find the two transition states, also using the same GFN1-xTB method. With these geometry optimizations, the free energies were calculated using a very similar equation to the binding energy equation for the glucose sensing portion:

$$Free\ Energy\ of\ Reaction\ (\Delta G) = G_{Total\ Rxn} - G_{Slab} \quad (3)$$

Free energies calculated for the full reaction (with the reaction over the slab) are subtracted by the free energy of the slab. This gives the free energy of the reaction, which follows the rule that the more negative it is, the more spontaneous the reaction is.

This mechanism also can be converted to DMO, so the same geometry optimizations were done to determine which product was more favored and compared to the experimental work, which had DMC favored over DMO (Fujinuma, 2022).

3.2.2 Computational Methods: Using DFTB in AMS Software

To create these slabs, they were periodic cells made using AMS (R. Rüger, 2023) as 4x4 layered slabs, with the 1 to 1 ratio slab having Miller Indices of (1, 1, 1) with the Au and Pd. For all optimizations, the method used was the GFN1-xTB DFTB method (Stefan Grimme, 2017) with a $1*10^{-5}$ Hartree optimization tolerance. The transition states were found using 2D reaction coordinate scans along the O-H and C-O bonds to locate the transition states and confirm them as the proper transition states.

For all calculations in this section, we employed DFTB (Density Functional Tight Binding) in place of the DFT (Density Functional Theory) used in our other studies. DFTB is different than DFT because it can be used in larger-scale simulations where DFT would fail. Some reasons why DFTB can be used on larger scales are because the atomic orbital basis set representations are more limited and straightforward in a sense where some parameters are a set approximation rather than part of a calculation that would be involved in DFT, such as the reference density $\rho(r)$ (Seifert, 2014). Those are a few examples, however, there are more details involved with the overall differences and improvements to DFT.

3.3 Computational Results and Discussion

3.3.1 Computational Results: Favoring DMC Over DMO and MF

To create the checkerboard slabs, different methods of making these different "bands" to match with experimental were done first. Some examples include slabs mostly of one metal with 3 or 4 atoms of the other at the surface and a Pd slab with 4 atoms of Au deposit on top. However, the checkerboard slab had shown the favored results and

was decided to be the slab to represent the mechanism. As stated above, optimizations were done to represent each step of the mechanism, which includes the reactants, products, an intermediate, and two transition states between the reactants and intermediate and between the intermediate and products. The second transition state had the DMC product used since it ended up being more favorable and matched the experimental work that way too (Fujinuma, 2022). Overall, in Figure 3.1, it is clear that in each step of the mechanism, the components tend to interact with the palladium (blue atoms) rather than the gold (yellow atoms). This lines up with previous knowledge of Au/Pd metal alloys, with stronger binding to Pd over Au (Mengyao Ouyang, 2021).

Figure 3.1

The Optimized Geometries for the Reaction Mechanism

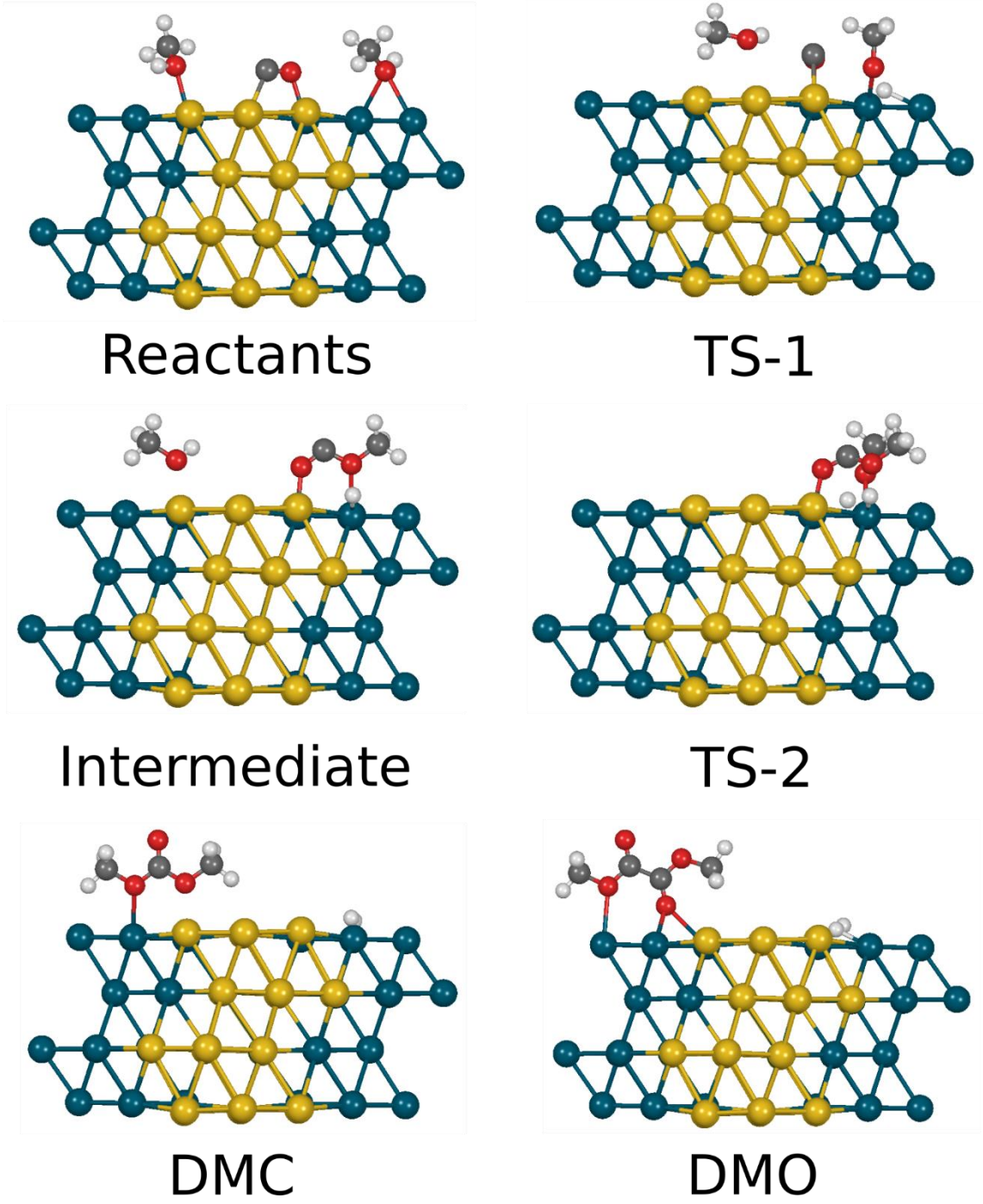

Based on the information in Figure 3.2, it is confirmed that the checkerboard slab (marked as CB in black) was the most desirable out of the three. With knowledge of alloys VS metals alone, that makes sense. The reason is that it's the most desired in both the moderate and weaker interactions, which could be more applicable than favoring only the highly adsorbed. However, as a highly absorbed reactant, Pd is the leading metal over the checkerboard slab. The Au slab is the least favored of all three interaction types, with all positive free energies.

Based on the structures in the mechanism, a majority of the steps are taking place over the Pd parts of the slab, which aligns with previous knowledge on Au/Pd slabs. In Ouyang et al., it was determined that CO-Pd was thermodynamically more stable than over Au (Mengyao Ouyang, 2021). The reactants are happening over both the Au and Pd, which differs from the previous works, but the structures are vastly different. The previous work had a very small percentage of Pd aggregating to the surface with a large percentage of Au. This work has a 50/50 ratio with far fewer atoms overall. This knowledge of stability over the Pd atoms can help explain most of the reaction mechanism taking place over Pd rather than Au. Au's performance in Figure 3.2 can also prove that Pd is preferred over Au based on each of the metals' free energy performances.

Figure 3.2

The Relative Free Energy Diagram for Each of the Three Slabs at (a) Highly Absorbed Reactants, (b) Moderately Absorbed Reactants, and (c) Weakly Absorbed Reactants

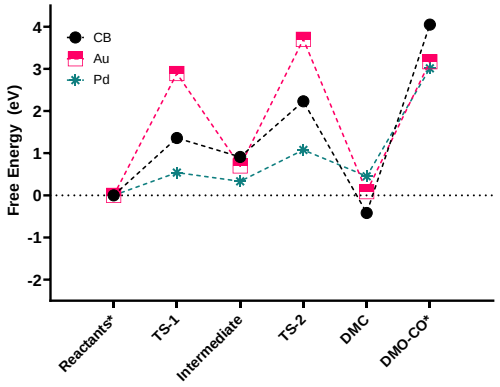

(a) Highly Absorbed

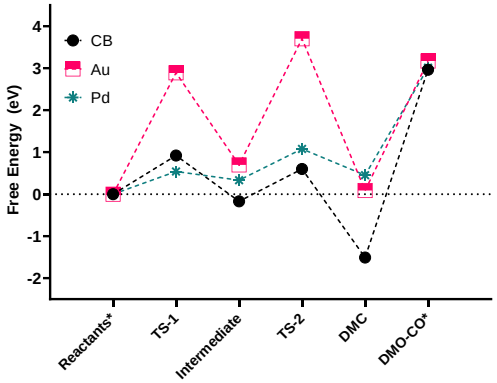

(b) Moderately Absorbed

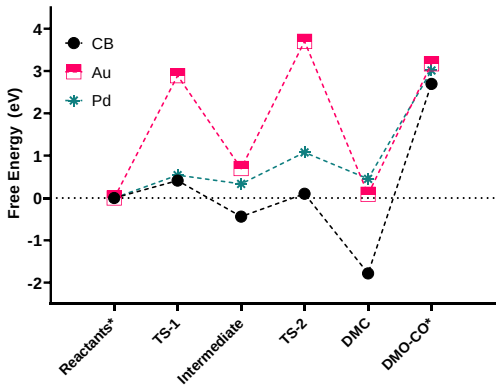

(c) Weakly Absorbed

3.3.2 Discussion

Based on the free energy diagrams, it is determined that DMC is the most favored product due to its very low free energies and DMO's very high free energies. This indicates in an electrocatalytic reaction, it will be easy to get to the product since it will happen spontaneously. On each slab, it is determined that the checkerboard slab is the most favorable, but the Pd slab can be useful in a highly absorbed case. A highly absorbed case can mean very close interactions, so it is not as efficient as the checkerboard slab because it requires very close interactions to work well. However, at moderate and weak interactions, the checkerboard slab is most desired. That indicates CO_2 molecules at farther distances would be reduced, which is more applicable than the Pd slab. Super close interactions would only be possible in a high-pressure environment, and CO_2 reduction would not be likely in that environment if it were to make it to a larger scale. The Au slab was deficient in all three cases, making it not applicable. In b and c, it is determined that the highest free energy is about 1 eV, which means it is very reasonable to run this electrocatalytic reaction.

As stated above, Pd seems to be the favored part of the alloy to interact with based on previous results and thermodynamics. In the mechanism, CO and methanol are the only two that fully bind to the Au while DMO, intermediates, and transition states, will partially bind to Au and Pd or strictly bind to Pd. This does indicate that Pd leads to binding and stability. Pd on its own is preferred over Au, which doesn't necessarily correlate because alloys act differently, but it does show that Pd is desired in both an alloy and on its own.

In the experimental work, it was determined that the Pd/Au mixture favors DMC over DMO and MF with a Faradaic Efficiency of up to 92%. The 50/50 Pd/Au alloy was also determined to be preferred based on a current increase in the cyclic voltammetry plots (Fujinuma, 2022).

Chapter 4

Conclusion and Future Outlooks

4.1 Conclusion

Overall, metal alloys are efficient catalysts for both electrocatalysts and glucose sensing. Based on binding energies and Fermi energies, Ni_3P was the favored glucose sensor with the most negative binding energy and least negative Fermi energy, confirming the strongest binding and proper electron transfer. It also had weak binding with different biomolecules. Ni_2P was the second desired and $Ni_{12}P_5$ was the least desired based on those two properties. Ni_2P binding with fructose also made sense with previous data. DOS/PDOS and BAND confirmed metallic properties and where the bandgap was located. Ni_3P hasn't been studied in glucose sensing and could be interesting to investigate more.

For electrocatalysis of CO_2 to DMC, it was determined that DMC was the preferred pathway based on the free energy differences over DMO. The checkerboard slab alloy had the most negative free energies of the three slabs, which makes sense knowing the properties of metal alloys over metals. The Pd sections had the most interactions over it throughout the mechanism. Au/Pd works efficiently as an electrocatalyst at strong, moderate, and weak interactions.

4.2 Future Outlooks

In glucose sensing, based on Ni_3P's electron delocalization properties, its glucose sensing properties, and binding energies to glucose VS other biomolecules, it would be

interesting to use Ni_3P in an experimental work. Also, with the computational power, more simulations with other catalytic sources, such as graphene. For the electrocatalytic reaction, different percentages of Au and Pd or different types of slabs other than the checkerboard slab would be interesting to study, with Pd's stronger binding to the reaction components.

References

Albisser, A. M., Leibel, B. S., Ewart, T. G., Davidovac, Z., Botz, C. K., Zingg, W., Schipper, H., & Gander, R. (1974). Clinical Control of Diabetes by the Artificial Pancreas. *Diabetes*, *23*(5), 397-404. https://doi.org/10.2337/diab.23.5.397

Alvarez-Galvan, M. C., Campos-Martin, J. M., & Fierro, J. L. G. (2019). Transition Metal Phosphides for the Catalytic Hydrodeoxygenation of Waste Oils into Green Diesel. *Catalysts*, *9*(3), 293. https://doi.org/10.3390/catal9030293

Anders B. Laursen, R. B. W., Marianna J. Whitaker, Edward J. Izett, Karin U. D. Calvinho, Shinjae Hwang, Ross Rucker, Hao Wang, Jing Li, Eric Garfunkel, Martha Greenblatt, Andrew M. Rappe, and G. Charles Dismukes. (2018). Climbing the Volcano of Electrocatalytic Activity while Avoiding Catalyst Corrosion: Ni3P, a Hydrogen Evolution Electrocatalyst Stable in Both Acid and Alkali. *ACS Catalysis*, *8*(5), 4408-4419. https://doi.org/10.1021/acscatal.7b04466

Antara Vaidyanathan, S. L., Gopal Sanyal, Saju Joseph, Nandakumar Kalarikkal, Brahmananda Chakraborty. (2021). Nitrobenzene sensing in pristine and metal doped 2D dichalcogenide MoS2: Insights from density functional theory investigations. *Applied Surface Science, 550.* https://doi.org/10.1016/j.apsusc.2021.149395

Arvind Jina, M. T., Janet A Tamada, Scott McGill, Shashi P. Desai, Beelee Chua, Anna Chang, and Mark Christiansen. (2014). Design, Development, and Evaluation of a Novel Microneedle Array-based Continuous Glucose Monitor. *Journal of Diabetes Science and Technology*, *8*(3), 483-487. https://doi.org/10.1177/1932296814526191

Association, A. D. (2007). Diagnosis and Classification of Diabetes Mellitus. *Diabetes Care*, *30*, S42-S47. https://doi.org/10.2337/dc07-S042

Burrin, J. M., & Price, C. P. (1985). Measurement of Blood Glucose. *Annals of Clinical Biochemistry*, *22*(4), 327-342. https://doi.org/10.1177/000456328502200401

Chunde Wang, T. D., Yuan Sun, Xiaoli Zhou, Yun Liua, and Qing Yang (2015). Ni12P5 nanoparticles decorated on carbon nanotubes with enhanced electrocatalytic and lithium storage properties. *Nanoscale, 7*(45), 19241-19249. https://doi.org/10.1039/C5NR05432J

Courtney A. Downes, K. M. V. A., Sean A. Tacey, Kinga A. Unocic, Frederick G. Baddour, Daniel A. Ruddy, Nicole J. LiBretto, Max M. O'Connor, Carrie A. Farberow, Joshua A. Schaidle, and Susan E. Habas. (2022). Controlled Synthesis of Transition Metal Phosphide Nanoparticles to Establish Composition-Dependent Trends in Electrocatalytic Activity. *Chemistry of Materials*, *34*(14), 6255-6267. https://doi.org/10.1021/acs.chemmater.2c00085

Daisuke Kanama, S. T. O., Shigeki Otani, David F Cox (2004). Photoemission and LEED characterization of Ni2P(0001). *Surface Science*, *552*(1-3), 8-16. https://doi.org/10.1016/j.susc.2004.01.038

Danielle Bruen, C. D., Larisa Florea, and Dermot Diamond. (2017). Glucose Sensing for Diabetes Monitoring: Recent Developments. *Sensors*, *17*(8). https://doi.org/10.3390/s17081866

Dong Zhang, X. Z., Jiaan Liu, Lina Dong, Jinpeng Zhao, Ying Xie, Weifeng Sun. (2021). Selective synthesis of Ni12P5 and Ni2P nanoparticles: Electronic structures, magnetic and optical properties. *Materials Science and Engineering*, *273*. https://doi.org/10.1016/j.mseb.2021.115389

E. Bekaert, J. B., S. Boyanov, L. Monconduit, M.-L. Doublet, and M. Ménétrier. (2008). Direct Correlation between the 31P MAS NMR Response and the Electronic Structure of Some Transition Metal Phosphides. *The Journal of Physical Chemistry*, *112*(51), 20481-20490. https://doi.org/10.1021/jp808122q

Emerging Risk Factors Collaboration 1; N Sarwar, P. G., S R Kondapally Seshasai, R Gobin, S Kaptoge, E Di Angelantonio, E Ingelsson, D A Lawlor, E Selvin, M Stampfer, C D A Stehouwer, S Lewington, L Pennells, A Thompson, N Sattar, I R White, K K Ray, J Danesh. (2010). Diabetes mellitus, fasting blood glucose concentration, and risk of vascular disease: a collaborative meta-analysis of 102 prospective studies. *PubMed*, *375*(9733), 2215-2222. https://doi.org/10.1016/S0140-6736(10)60484-9

Fujinuma, N. (2022). *Development of Synergistic Electrochemical Catalysis for Advancing CO2 Utilization* Rowan University.

Giannozzi P, A. O., Brumme T, Bunau O, Buongiorno Nardelli M, Calandra M, Car R, Cavazzoni C, Ceresoli D, Cococcioni M, Colonna N, Carnimeo I, Dal Corso A, de Gironcoli S, Delugas P, DiStasio RA Jr, Ferretti A, Floris A, Fratesi G, Fugallo G, Gebauer R, Gerstmann U, Giustino F, Gorni T, Jia J, Kawamura M, Ko HY, Kokalj A, Küçükbenli E, Lazzeri M, Marsili M, Marzari N, Mauri F, Nguyen NL, Nguyen HV, Otero-de-la-Roza A, Paulatto L, Poncé S, Rocca D, Sabatini R, Santra B, Schlipf M, Seitsonen AP, Smogunov A, Timrov I, Thonhauser T, Umari P, Vast N, Wu X, Baroni S. . (2017). Advanced capabilities for materials modelling with Quantum ESPRESSO. *J Phys Condens Matter*, *29*(46). https://doi.org/10.1088/1361-648X/aa8f79

Harald Ibach , H. L. (2009). *Solid-State Physics, An Introduction to Principles of Materials Science* (4 ed.). Springer Berlin, Heidelberg. https://doi.org/10.1007/978-3-540-93804-0

Hassan, F. E. H. (2015). General Electronic Theory. In *Electronic and vibrational theory of crystals*. Lebanese University. https://doi.org/10.13140/2.1.4369.3129

Hendrik J.R. Lemmer, W. L. (2022). Crystallization: Its Mechanisms and Pharmaceutical Applications. In *Crystal Growth - Technologies and Applications*. https://doi.org/10.5772/intechopen.105056

Jain, A., Ong, S. P., Hautier, G., Chen, W., Richards, W. D., Dacek, S., Cholia, S., Gunter, D., Skinner, D., Ceder, G., & Persson, K. A. (2013). Commentary: The Materials Project: A materials genome approach to accelerating materials innovation. *APL Materials*, *1*(1). https://doi.org/10.1063/1.4812323

John P. Perdew, K. B., and Matthias Ernzerhof. (1996). Generalized Gradient Approximation Made Simple. *Phys. Rev. Lett.*, *77*(18), 3865-3868. https://doi.org/10.1103/PhysRevLett.77.3865

Kahn, A. (2016). Fermi level, work function and vacuum level. *Materials Horizons*, *3*(7). https://doi.org/10.1039/C5MH00160A

Leland C. Clark, J., Champ Lyons. (1962). Electrode systems for continuous monitoring in cardiovascular surgery. *Ann. N.Y. Acad. Sci.*, *102*, 29-45. https://doi.org/10.1111/j.1749-6632.1962.tb13623.x

Liangcai Zhou, Y. K., Yong Du, Jiong Wang, Yichun Zhou. (2010). Spatial and electronic structure of the Ni3P surface. *Applied Surface Science*, *256*(24), 7692-7695. https://doi.org/10.1016/j.apsusc.2010.06.038

M. Bursch, J.-M. M., A. Hansen, S. Grimme (2022). Best-Practice DFT Protocols for Basic Molecular Computational Chemistry. *Angewandte Chemie*, *61*(42). https://doi.org/10.1002/anie.202205735

Masson-Delmotte, V., P. Zhai, A. Pirani, S.L. Connors, C. Péan, S. Berger, N. Caud, Y. Chen, L. Goldfarb, M.I. Gomis, M. Huang, K. Leitzell, E. Lonnoy, J.B.R. Matthews, T.K. Maycock, T. Waterfield, O. Yelekçi, R. Yu, and B. Zhou (eds.). (2021). *Climate Change 2021: The Physical Science Basis. Contribution of Working Group I to the Sixth Assessment Report of the Intergovernmental Panel on Climate Change*. C. Cambridge University Press, United Kingdom and New York, NY, USA, In press. https://doi.org/10.1017/9781009157896

Mengyao Ouyang, K. G. P., Alexey Boubnov, Adam S. Hoffman, Georgios Giannakakis, Simon R. Bare, Michail Stamatakis, Maria Flytzani-Stephanopoulos & E. Charles H. Sykes. (2021). Directing reaction pathways via in situ control of active site geometries in PdAu single-atom alloy catalysts. *Nature Communications*, *12*. https://doi.org/10.1038/s41467-021-21555-z

Mingzhu Wang, X. W., Shiya Feng, Daiping He, and Ping Jiang. (2020). Amorphous Ni-P nanoparticles anchoring on nickel foam as an efficient integrated anode for glucose sensing and oxygen evolution. *Nanotechnology, 31*, Article 45. https://doi.org/10.1088/1361-6528/abab30

Naikoo, G. A., Salim, H., Hassan, I. U., Awan, T., Arshad, F., Pedram, M. Z., Ahmed, W., & Qurashi, A. (2021). Recent Advances in Non-Enzymatic Glucose Sensors Based on Metal and Metal Oxide Nanostructures for Diabetes Management- A Review [Review]. *Frontiers in Chemistry*, *9*. https://doi.org/10.3389/fchem.2021.748957

Pandey, A. T., Poonam; Pandey, Rishabh; Srivatava, Rashmi; Goswami, Shambaditya. (2011). Alternative therapies useful in the management of diabetes. https//doi.org/10.4103/0975-7406.90103

A systematic review. *Journal of Pharmacy and Bioallied Sciences*, *3*(4), 504-512. https://doi.org/10.4103/0975-7406.90103

Paolo Giannozzi, S. B., Nicola Bonini, Matteo Calandra, Roberto Car, Carlo Cavazzoni, Davide Ceresoli, Guido L Chiarotti, Matteo Cococcioni, Ismaila Dabo, Andrea Dal Corso, Stefano de Gironcoli, Stefano Fabris, Guido Fratesi, Ralph Gebauer, Uwe Gerstmann, Christos Gougoussis, Anton Kokalj, Michele Lazzeri, Layla Martin-Samos, Nicola Marzari, Francesco Mauri, Riccardo Mazzarello, Stefano Paolini, Alfredo Pasquarello, Lorenzo Paulatto, Carlo Sbraccia, Sandro Scandolo, Gabriele Sclauzero, Ari P Seitsonen, Alexander Smogunov, Paolo Umari, Renata M Wentzcovitch. (2009). Quantum ESPRESSO: A modular and open-source software project for quantum simulations of materials. *J. Phys.: Condens. Matter*, *21*(39). https://doi.org/10.1088/0953-8984/21/39/395502

Paul, R. K. S. a. S. (2019). Metal Complexes in Medicine: An Overview and Update from Drug Design Perspective. *Cancer Therapy and Oncology International Journal*, *14*(1). https://doi.org/10.19080/CTOIJ.2019.14.555883

Peter Kratzer, a. J. N. (2019). The Basics of Electronic Structure Theory for Periodic Systems. *Frontiers in Chemistry*, *7*(106). https://doi.org/10.3389/fchem.2019.00106

R. Rüger, M. F., T. Trnka, A. Yakovlev, E. van Lenthe, P. Philipsen, T. van Vuren, B. Klumpers, T. Soini. (2023). *AMS 2023.1, SCM, Theoretical Chemistry*. In http://www.scm.com

S. Jelev-Vlaev, R. d. C., A. Del R´ıo de Santiago, and J. C. Mart´ınez-Orozco. (2009). Total Density of States in Rectangular Quantum Wells. *Piers Online, 5*(2). https://doi.org/10.2529/PIERS080908020543

S. R. Corrie, J. W. C., J. Islam, K. A. Markey and M. A. F. Kendall (2015). Blood, sweat, and tears: developing clinically relevant protein biosensors for integrated

body fluid analysis. *Analyst*, *140*, 4350-4364. https://doi.org/10.1039/C5AN00464K

Schrödinger Release 2023-4: Maestro, S., LLC, New York, NY, 2023.

Schrödinger Release 2023-4: Materials Science Suite, S., LLC, New York, NY, 2023.

Seetha Lakshmy, S. S., Nandakumar Kalarikkal, Chandra Sekhar Rout, Brahmananda Chakraborthy. (2023). A review of electrochemical glucose sensing based on transition metal phosphides. *Journal of Applied Physics*, *133*(7). https://doi.org/10.1063/5.0111591

Seifert, M. E. a. G. (2014). Density functional tight binding. *Philosophical Transactions of the Royal Society A, 372*. https://doi.org/10.1098/rsta.2012.0483

Shu Fujita, K. N., Jun Yamasaki, Tomoo Mizugaki, Koichiro Jitsukawa, and Takato Mitsudome. (2020). Unique Catalysis of Nickel Phosphide Nanoparticles to Promote the Selective Transformation of Biofuranic Aldehydes into Diketones in Water. *ACS Catalysis*, *10*(7), 4261-4267. https://doi.org/10.1021/acscatal.9b05120

Shulin Zhao, S. L., Tao Guo, Shuaishuai Zhang, Jing Wang, Yuping Wu, Yuhui, & Chen. (2019). Advances in Sn-Based Catalysts for Electrochemical CO2 Reduction. *Nano-Micro Letters*, *11*. https://doi.org/10.1007/s40820-019-0293-x

Stefan Grimme, C. B., and Philip Shushkov. (2017). A Robust and Accurate Tight-Binding Quantum Chemical Method for Structures, Vibrational Frequencies, and Noncovalent Interactions of Large Molecular Systems Parametrized for All spd-Block Elements (Z = 1–86). *Journal of Chemical Theory and Computation*, *13*(5), 1989-2009. https://doi.org/10.1021/acs.jctc.7b00118

Tania P. Brito, N. B.-M., Andrónico Neira-Carrillo, Soledad Bollo, and Domingo Ruíz-León. (2022). Synergistic Effect of Composite Nickel Phosphide Nanoparticles and Carbon Fiber on the Enhancement of Salivary Enzyme-Free Glucose Sensing. *Biosensors*, *13*(49). https://doi.org/10.3390/bios13010049

Tanja van Mourik, M. B., and Marie-Pierre Gaigeot. (2014). Density functional theory across chemistry, physics and biology. *Philos Trans A Math Phys Eng Sci*, *372*. https://doi.org/10.1098/rsta.2012.0488

Tao Chen, D. L., Wenbo Lu, Kunyang Wang, Gu Du, Abdullah M Asiri, Xuping Sun. (2016). Three-Dimensional Ni2P Nanoarray: An Efficient Catalyst Electrode for Sensitive and Selective Nonenzymatic Glucose Sensing with High Specificity. *Analytical Chemistry*, *88*(16), 7873-8346. https://doi.org/10.1021/acs.analchem.6b02216

Tarr, G. L. M. a. D. A. (1999). *Inorganic Chemistry* (2, Ed.). Pearson Education. https://doi.org/10.1007/s00897990322a

Tran Thanh Tam Toan, D. M. N., Anh Quang Dao, Van Thuan Le, Yasser Vasseghian. (2023). Latest insights on metal-based catalysts in the electrocatalysis processes: Challenges and future perspectives. *Molecular Catalysis*, *538*. https://doi.org/10.1016/j.mcat.2023.113001

Villena Gonzales W, M. A., Abbosh A. (2019). The Progress of Glucose Monitoring-A Review of Invasive to Minimally and Non-Invasive Techniques, Devices and Sensors. *Sensors*, *19*(4). https://doi.org/10.3390/s19040800

VIVEK N AMBADE, Y. S., and BL SOMANI, Dr. (1998). METHODS FOR ESTIMATION OF BLOOD GLUCOSE : A COMPARATIVE EVALUATION. *Med J Armed Forces India*, *54*(2). https://doi.org/10.1016/S0377-1237(17)30502-6

Yang Hea, J.-C. L., Langli Luod, Yang-Gang Wangb, Junfa Zhue, Yingge Dug, Jun Li (李隽), Scott X. Maoa, and Chongmin Wang. (2018). Size-dependent dynamic structures of supported goldnanoparticles in CO oxidation reaction condition. *Proc Natl Acad Sci USA 115*(30), 7700-7705. https://doi.org/10.1073/pnas.1800262115

Zhiqun Ran, C. S., Zhiqian Hou, Weibin Zhang, Yu Yan, Miao He, Jianping Long. (2021). Modulating electronic structure of honeycomb-like Ni2P/Ni12P5 heterostructure with phosphorus vacancies for highly efficient lithium-oxygen batteries. *Chemical Engineering Journal*, *413*. https://doi.org/10.1016/j.cej.2020.127404